ELSEVIER

Hearing Research 136 (1999) 49–64

HEARING RESEARCH

The role of intermodulation distortion in transient-evoked otoacoustic emissions

Graeme K. Yates *, Robert H. Withnell

The Auditory Laboratory, Department of Physiology, The University of Western Australia, Nedlands, WA 6907, Australia

Received 25 December 1998; received in revised form 24 May 1999; accepted 6 June 1999

Abstract

Transient-evoked otoacoustic emissions (TEOAEs) are low-intensity sounds recorded in the external ear canal immediately following stimulation by a transient stimulus, typically a click. While the details of their production is unknown, there is evidence to suggest that the amplitude of each component frequency reflects the physiological condition of the corresponding region of the cochlea. Certain observations are at variance with this assumption, however, suggesting that pathology at a basal site within the cochlea might affect the production of emissions at frequencies which are not characteristic for that site. We have recorded click-evoked emissions in guinea pigs using high-pass clicks and found emissions at frequencies which are not present in the stimulus and which could not, therefore, have originated from the characteristic place for those emission frequencies. These new frequencies are, by definition, intermodulation distortion frequencies and must have been generated from combinations of frequencies in the stimulus by non-linear processes within the cochlea. Further processing of the emissions by Kemp's technique of non-linear recovery showed that the magnitude of emissions at frequencies within the stimulus frequency pass-band was approximately the same as that of frequencies not present in the stimulus. We propose that, in guinea pigs at least, most of the click-evoked emission energy is generated as intermodulation distortion, produced by non-linear intermodulation between various frequency components of the stimulus. If this result is confirmed in humans, many of the anomalies in the literature may be resolved.

Key words: Click-evoked otoacoustic emission; Non-linearity; Intermodulation distortion

1. Introduction

It is now more than 20 years since Kemp (1978) first described sounds re-emerging from within the inner ear in response to click stimuli, a phenomenon which has become widely known as the Kemp echo and, more recently, as the acoustically evoked otoacoustic emission (AEOAE). Kemp's motivation in searching for such echos was the presence of ripples in the audiogram (Elliott, 1958; van den Brink, 1970), which suggested to him that there might be reflections of the travelling wave present in the cochlea. More recent studies have shown that these and related, low-intensity phenomena are associated with the cochlear amplifier. A variety of other, related emissions have also been described: spontaneous (Strickland et al., 1985), stimulus frequency (Souter, 1995) and distortion product (Kim et al., 1980; Kemp and Brown, 1984). In spite of many years of intensive investigation, no clear understanding of the mechanism of otoacoustic emission generation exists to date.

Kemp reasoned that low-level stimulation of an active source of mechanical power, close to the place of greatest mechanical response, might cause a partial reflection of energy from the stimulus travelling wave, returning some of the input energy to the external ear (Kemp, 1986). In other words, he suggested the possibility of an impedance change which might lead to a reflection. Other authors have made alternative suggestions. Strube (1989) claimed that simple wave-based reflections are impossible and proposed that emissions may be due to Bragg reflections from some place-fixed,

* Corresponding author. Tel.: +61 (8) 9380 3321; Fax: +61 (8) 9380 1025; E-mail: gyates@cyllene.uwa.edu.au

0378-5955/99/$ – see front matter
PII: S0378-5955(99)00108-2

quasi-periodic irregularities in the mechanical properties of the basilar membrane (BM), possibly in the outer hair cells (Manley, 1983). To date, however, no physiological basic for such irregularities has been found. Furthermore, Shera and Zweig (1993) observed that such Bragg reflections should result in cyclic variations of the reflection travelling wave ratio, for which they found no evidence. They then argued (Shera and Zweig, 1993; Zweig and Shera, 1995) for similar reflections but suggested that the reflections may be from random irregularities which were effective only in the maximum amplitude region of the travelling wave. In their model, the threshold microstructure is due to cyclic variation of the phase between the forward and reverse travelling waves at the stapes.

Many authors have assumed that the click-evoked emission is simply a superposition of many, simultaneous stimulus frequency responses to the wide-band stimulus. Inherent in this assumption is the concept of the 'emission channel' in which it is assumed that each frequency component present in an emission response is the direct result of stimulation with that same frequency. That is, the presence in the emission of a particular frequency f implies both the presence of f in the stimulus and the normal operation of the cochlear amplifier at the characteristic place for f. Each f is assumed to operate within its own 'channel'. This assumption has been tested several times, always with a positive outcome. Norton and Neely (1987) used Blackman-filtered tone bursts and found a close, but not exact, correspondence between stimulus and response spectra in humans, concluding that the emission originated at a site appropriate to the stimulus frequency. Xu et al. (1994), again in humans, used the principle of superposition by comparing the responses to independent tone bursts of 1, 2 and 3 kHz with the response when all three-tone bursts were presented together. They found that the sum of the responses to the individual tones was approximately equal to the response to the three-tone stimulus and concluded that the stimulus was analyzed by independent channels. It is difficult to see, however, how any other result could have been obtained. The peaks in the travelling waves due to the three frequencies would have been well-separated on the BM so there would have been little possibility for interaction and therefore little possibility for differences to arise. In a more realistic test, Prieve et al. (1996) compared click-evoked transient-evoked otoacoustic emissions (TEOAEs) filtered into 1/3rd octave bands with emissions produced by Blackman-filtered tone bursts. Again, they found a close correspondence and concluded that the respective frequency components of TEOAEs were processed on separate channels. A possible weakness with their study, however, relates to the bandwidth of their 'narrow-band' stimuli which were close to one octave wide. It is possible that their stimuli were too broad to provide an adequate approximation to a single channel stimulus.

Such experiments lend some support to the independent channel model, but other observations are more difficult to reconcile with such a concept. Hilger et al. (1995) recorded click-evoked emissions in guinea pigs and unsuccessfully attempted to correlate them with structural anomalies on the BM. The only correlation they could find was with the total number of outer hair cells missing and they concluded that TEOAEs were not a result of reflection from outer hair cell pathologies on the organ of Corti. They were more likely the result of mild irregularities along the cochlear partition, as suggested by Shera and Zweig.

Results from suppression experiments are also at odds with the general ideas of TEOAE production. In an independent channel model, it should be possible to suppress TEOAEs over a narrow range of frequencies by introducing a simultaneous tone at a moderate intensity. Such a tone will stimulate only a very narrow region of the BM and so will suppress the cochlear amplifier at a specific site. This should then, according to the independent channel model, result in a notch in the emission spectrum centered on the suppressor frequency. Kemp and Chum (1980) did in fact report such an observation, but with the qualification that such a suppression occurred only when the suppressor frequency was set at a peak in the emission frequency. Sutton (1985) used a single cycle of a 2 kHz sine wave as a stimulus and recorded emissions in his own ear, with and without suppressor tones. While suppression effects were generally strongest at frequencies relatively close to and below the suppressor, several regions of the emission spectrum were suppressed even by fairly remote suppressors. He concluded that the emission generators were not simply localized sources but were distributed over a considerable length of the cochlea. Withnell and Yates (1998) attempted to suppress click-evoked emissions in guinea pigs using pure tones and found very little frequency-specific suppression and more usually, non-specific enhancement over a wide-band of the emission spectrum. They suggested that the emission, far from being channel-specific, might actually consist mostly of intermodulation distortion.

A final problem for the independent channel model of TEOAE production exists in the studies by Avan et al. (1993, 1995, 1997). TEOAEs typically are restricted to the frequency range below 6 kHz and under existing assumptions about TEOAE production, they should be independent of the hearing status above 6 kHz. In their first study, Avan et al. (1993) compared TEOAEs from normal hearing subjects with those from subjects with high-frequency hearing loss. They found significant changes in the emission waveforms from the damaged

ears, even for frequency components well below the frequencies of the hearing impairment. They concluded that the basal region of the cochlea had a significant role in the production of low-frequency components of the TEOAE. In their 1995 study, they compared TEOAEs in guinea pigs before and after acoustic trauma and found significant correlations between the emission spectral amplitudes (which are all below 6 kHz) and the damage to the basal turn of the cochlea. Again, they suggested the possibility that the basal turn played a role in production of low-frequency TEOAE components. Finally, in their 1997 paper, they reported correlations between human, click-evoked TEOAEs and hearing thresholds over the range 8–16 kHz and suggested that variations in high-frequency hearing status might be responsible for at least a part of the variance of normal emission data.

In view of the considerable disagreement in the literature on the frequency-specificity of TEOAEs and given their now wide-spread use in clinical audiology and screening, it is essential that we have a more fundamental understanding of the mechanism by which they are generated. To this end, we have examined click-evoked emissions in guinea pigs using a highly linear sound system. Reports in the literature suggest that TEOAEs in guinea pigs are very small (Hilger et al., 1995) and other differences between emissions from humans and guinea pigs have been noted (Brown and Gaskill, 1990). Given the potential for intervention in acute animal experiments, however, it would seem that animal experiments might be the better way to study the problem. We now report results of experiments on guinea pigs which provide clear evidence in support of the notion that TEOAEs consist mostly of intermodulation products generated by non-linear interactions between the component frequencies of the stimulus. Our conclusions are based on measurements of emissions made using steeply filtered clicks which permitted examination of emission frequencies within and outside of the stimulus frequency band.

2. Materials and methods

2.1. Stimulus generation and recording

From the outset, it appeared to us that we would require a stimulus generation and sound recording system that was as linear as possible, since existing instrumentation systems generate their own distortion which necessitates windowing out the early components of the emission. We therefore chose not to use the usual, commercially available AEOAE systems and instead to construct a custom system to our own design. All sound generation and recording was carried out using a sound card (Crystal Semiconductors CS4231/4248) which conforms to the standard for the Microsoft Windows 95 Sound System and all software was written using standard operating system calls. The maximum sampling rate is limited to 48 000 s^{-1} but we always used 44 100 s^{-1}, so the maximum frequency which may be generated or recorded, allowing for the anti-aliasing filters, is approximately 20.5 kHz.

The acoustic stimulus was generated by a 16 mm diameter loudspeaker (Foster Electric, Japan, dynamic earphone type T016H01A0000) placed approximately 15 mm from the meatus (see below). No attempt at enclosing the speaker was made, so it was an open, almost free-field, stimulator. Sound was recorded by a Sennheiser MKE-2 microphone fitted with an electrically insulated metal probe tube (9 mm long, 1.3 mm in diameter, 1500Ω acoustic resistor), followed by a custom-made, low-noise, highly linear amplifier. The microphone and probe tube combination was calibrated against a Bruel and Kjaer 1/8 inch microphone. Signals from the amplifier were high-pass filtered at 300 Hz and transmitted as a differential input to the stereo channels of the computer sound card. Software subtracted the right channel from the left, reducing computer bus and common mode interference by at least 10 dB.

The stimulus waveform was calculated as a sinc function (sin (x)/x), appropriately time-scaled according to the required low-pass frequency and windowed over ± 1.5 ms, using the equation

$$\begin{aligned} a(t) &= \cos^2(\pi t/0.003)\frac{\sin(2\pi f_c t)}{2\pi f_c t} && -0.0015; < t < 0.0015 \\ &= 0 && \text{otherwise} \end{aligned}$$

where f_c is the low-pass corner frequency. The waveform was then shifted by 2 ms so that the peak was centered on $t = 2$ ms. The windowing function is required to restrict the temporal extent of the stimulus, but it results in some degrading of the 'brick wall' nature of the cut-off in the frequency domain. When a band-pass click having a lower frequency bound of f_l and an upper frequency bound of f_h was required, it was computed by subtracting an appropriately scaled low-pass click of corner frequency f_l from a similar click of frequency limit f_h. Fig. 1 shows examples of electrical waveforms used and their spectra. In a later discussion, we will refer to high-pass and low-pass clicks, but in no case were the clicks actually passed through an electronic filter: the waveform was calculated explicitly when the click was generated.

Electrical signals from the probe microphone were digitized, averaged and automatically corrected for probe tube characteristic, both in amplitude and phase. Non-linear differential emissions were calculated following Bray and Kemp (1987). A train of clicks was

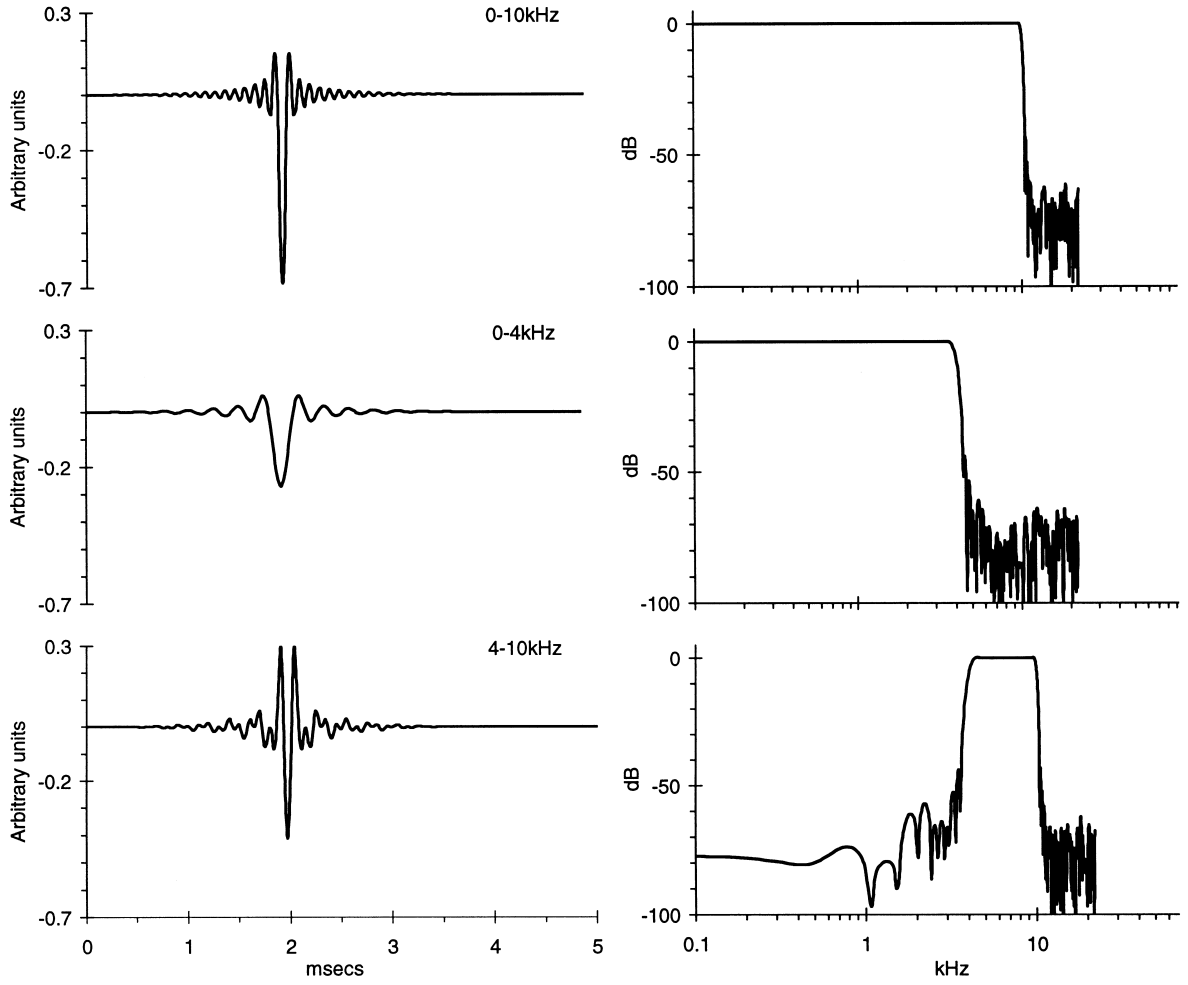

Fig. 1. Three examples of band-limited click waveforms measured by looping back the electrical output signal to the input of the computer sound card. Left: top panel, 0–10 kHz. Middle panel, 0–4 kHz. Bottom panel, 4–10kHz. Ordinate units are arbitrary linear units. Right: the corresponding spectra. The 4–10 kHz click is calculated by simple subtraction, in the time domain, of the 0–4 kHz click from the 0–10 kHz click. Ordinate units are dB.

presented, several at one intensity followed by a single click at a higher intensity. The number of softer clicks was equal to the ratio between their nominal peak pressure and that of the otherwise identical louder click. Ear canal sound waveforms in response to the two click types were recorded, separately, and then the loud click was subtracted from the sum of the softer clicks. In a linear system, the result should be simply noise, but in the ear canal of a normally hearing animal or human, a clear response, called the non-linear derived emission, is found. When referring to the two clicks, we will call the louder click the reference and the softer click the probe. Power spectral densities were computed for intervals of 1024 bins or 23.22 ms. Half-cosine windowing was applied to the time domain records over the first and last 2 ms of each record, so that almost none of the stimulus was windowed out.

In later experiments, the stimulus was adjusted to compensate for the frequency response of the stimulus sound system. To do this, the sound field was recorded in the meatus during stimulation with a pseudo-random noise signal computed by summing sine waves of discrete frequencies equally spaced from 43.07 to 21.65 kHz in steps of 43.07 Hz and with randomized phases. The impulse response of the stimulus system was then calculated from the recorded response. When we wanted to compensate a stimulus, the computed stimulus waveform was deconvolved with the impulse response from the noise stimulus to produce a waveform which, when played in the normal way, resulted in the desired waveform in the meatus. In this way, stimulus waveforms with a virtually flat frequency response and linear phase delay could be produced, although for technical reasons, the minimum high-pass frequency was limited to 1 kHz. Since the compensation technique is new to emission recording, we have included examples of both compensated and uncompensated clicks.

2.2. Animals and surgery

13 Healthy guinea pigs weighing between 450 and 750 g were used. They were anaesthetized with nembutal (30–35 mg/kg intraperitoneal (i.p.)) and atropine (0.06 mg i.p.), followed approximately 15 min later with leptan (0.15–0.2 ml intramuscular (i.m.)), following the neurolept anaesthesia technique of Evans (1979). Supplementary doses of nembutal and leptan were administered as required. Animals were tracheostomized and artificially ventilated on carbogen (5% CO_2, 95% O_2) while the rectal temperature was maintained at 37°C. The muscle relaxant alloferin (0.15 ml i.m.) was administered to inhibit spontaneous middle ear contractions and the heart rate was subsequently monitored. A silver wire electrode was placed on the bony ridge in front of the round window, through a small hole opened dorso-laterally in the bulla. Compound action potentials recorded by the electrode were used to monitor auditory thresholds and thereby judge the auditory stability of the preparation. The probe microphone was inserted approximately 2 mm into the external auditory meatus, leaving an approximately annular opening between the 1.8 mm o.d. of the probe tube and the 2.0–2.2 mm diameter of the meatus. We have shown this technique to be effective in recording otoacoustic emissions (Withnell et al., 1998). The loudspeaker supported the pinna and was placed approximately 1.5 cm from and just forward of the meatus (see Withnell et al., 1998 for details).

All experimental protocols were approved by the Animal Ethics and Experimentation Committee of the University of Western Australia (approval number UWA 91/97) and conformed with the Code of Practice of the National Health and Medical Research Council.

3. Results

3.1. Stimulus waveform

Adjustments of the stimulus waveform in order to compensate for the frequency response characteristics of the sound system were, in general, very successful. Uncompensated stimuli, although substantially flat over most of the frequency range from 1 to 20 kHz, showed variations of as much as 20 dB, typically around 7–10 kHz where a resonance in the loudspeaker caused a peak in the spectrum. Compensation resulted in an almost complete flattening of the spectrum and a shortening of the impulse waveform. Throughout this report, examples of responses to both compensated and uncompensated stimuli are presented. The compensated are more useful in quantitative comparisons but, since this work relies heavily on accurate stimulus control, the uncompensated are included to validate the compensation process.

In the time domain (Fig. 2a), the uncompensated sound stimulus started at approximately 2 ms after the recording epoch started, due to delays in the software, hardware anti-aliasing filters and propagation through the air, and showed some ringing at approximately 6–10 kHz which lasted for about 1.5 ms. For the waveform shown (the softer, probe click), the peak amplitude is 0.67 Pa. The power spectrum (Fig. 2c) is approximately flat up to 19.5 kHz, with a peak of about 14 dB between 6 and 10 kHz which is primarily responsible for the ringing in the time domain. Although the click amplitude is quite large, the duration is short and the overall energy is small, but peak amplitude is not very useful as an indicator of the cochlear stimulation anyway, since it varies greatly with the bandwidth and phase distortion. We cannot estimate the vibration amplitude produced on the BM, but it is much smaller than would be produced by a pure sine wave of equivalent peak pressure. Noise levels, determined by repeating the recording with the stimulus muted, were very low and are shown in Fig. 2d. The reference click appears identical (apart from a scaling factor) at the resolution of Fig. 2a and so is not included here.

3.2. Emissions

Fig. 2b shows the non-linear differential response for the same probe click. The emission starts at about the same time as the stimulus but rises more slowly. It then 'rings' for about 1.5 ms and abruptly ceases, leaving a much smaller amplitude response which continues significantly longer. The peak amplitude of the response is about 8 mPa, much larger than previously seen in the guinea pig (0.5 mPa: Avan et al., 1995; Hilger et al., 1995), although the later response, after about 1.5 ms from the onset of the stimulus, is of the same order as previously seen.

Similar results for a compensated click are also shown in Fig. 2e and f. The compensated (1–18 kHz) stimulus is now quite short and looks very similar to the desired click shapes shown in Fig. 1 but the emission has much the same duration as the uncompensated emission. The stimulus spectrum (g) is flat from 1 to 18 kHz with no sign of the sharp peak seen in the uncompensated click and falls off rapidly above and below the click band limits. The emission spectra (d, h), however, are not fundamentally different. Traces showing the spectra of the noise, recorded with the stimulus muted, are included in (d) and (h).

For these and all similar spectra shown here, the abscissa is labelled in dB re $(20\ \mu Pa)^2$/Hz and represents the power in each bin expressed relative to 400 μPa^2/Hz.

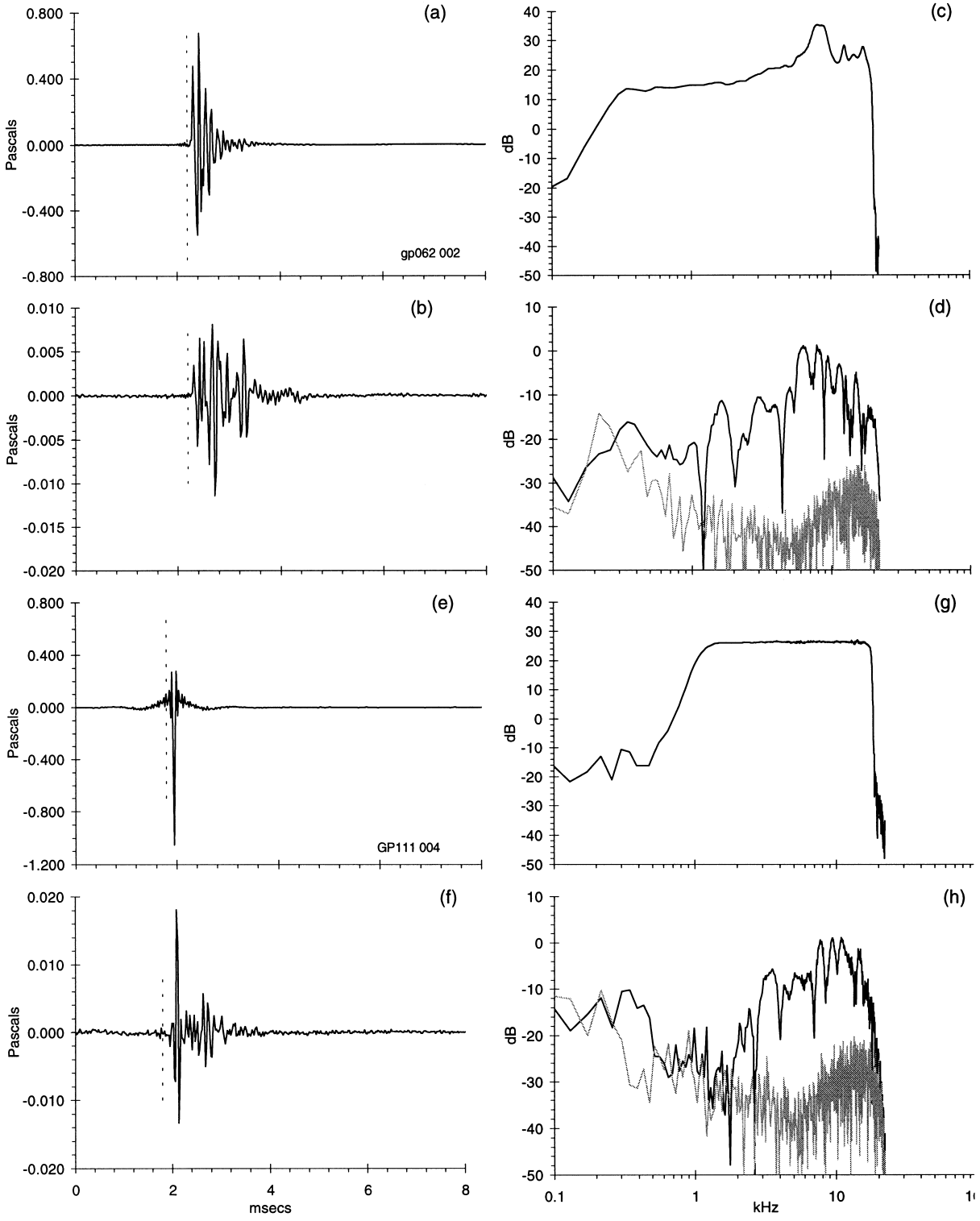

Fig. 2. Probe stimulus click and emission recorded in the external auditory meatus of a guinea pig and derived otoacoustic emission. (a) Uncompensated probe click. RMS pressure averaged over 23 ms is 35 mPa. (b) Emission derived from (a). (c) Power spectrum of (a). (d) Power spectrum of (b). (e–h) are similar, but for a click which has been compensated for the frequency response of the sound delivery system. RMS pressure averaged over 23 ms is 43 mPa. Reference click was 9 dB louder than the probe in each case. The thin, gray lines are the noise traces. Ordinate units are Pa for time domain responses, dB re $(20\ \mu Pa)^2$/Hz for frequency domain responses. The vertical, dotted lines in a and b and in e and f mark the same time points for comparison. Only the first 8 ms of the time traces are shown, but 23.22 ms was analyzed.

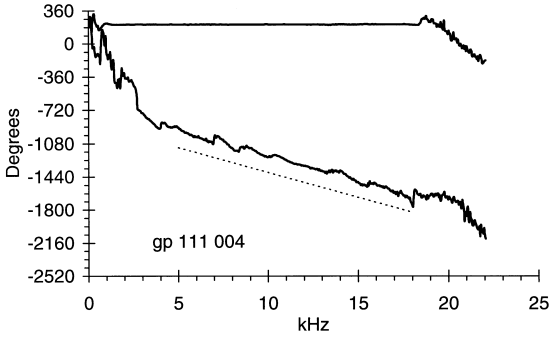

Fig. 3. Phase versus frequency for a wide-band, frequency-compensated click. The top line is the phase for the stimulus and is effectively flat, after subtraction of the 1.95 ms delay evident in Fig. 2e. The high and low frequency regions of significant slope are outside the nominal band limits of the click. The lower curve is the phase of the recovered emission. The straight, dotted line segment indicates a slope of 150 μs.

3.3. Emission phase

Fig. 3 shows the phase of both the ear canal sound pressure and the emission from the compensated stimulus of Fig. 2e and f, after subtraction of a delay of 1.95 ms. The stimulus phase is almost perfectly flat in the region over which it was compensated (1–18 kHz) but shows definite phase lags outside that range. The emission phase, however, is significantly steeper and substantially straight, representing a delay of about 150 μs over most of the bandwidth of the click.

3.4. Responses to high-pass clicks

We repeated the experiments with 4 kHz high-pass clicks. Since there is no power in the frequency band below 4 kHz, we should, under the channel-specific model, expect to find no power in the emission below 4 kHz. Fig. 4 shows the results for an uncompensated, high-pass click delivered to the same guinea pig as for Fig. 2a–c. In the curve marked (a), we show the measured spectrum of the ear canal sound pressure in response to the high-pass probe click. The thicker, gray line (b) is the expected spectrum, calculated by multiplying the spectrum of the wide-band probe click of Fig. 2c by the frequency characteristic for the high-pass click measured by hardware loopback. This is the spectrum we would expect from a simple, linear system. (c) is the system noise level. It is important to note that no processing has been carried out on these data other than the calculation of the Fourier transform and in particular, these are not spectra of non-linear differential emissions. What is dramatically evident in curve (a) is the existence of considerable power in the frequency band 800–4000 Hz which was not present in the electrical stimulus and which is well above the noise. It is, by definition, intermodulation distortion and is only some 40 dB below the magnitude of the stimulus itself. Fig. 5 shows a similar spectrum for a compensated click, although in this case, the expected signal is actually the uncompensated electrical stimulus looped back to the input and shifted vertically to align with the sound spectrum. Again, there is considerable power

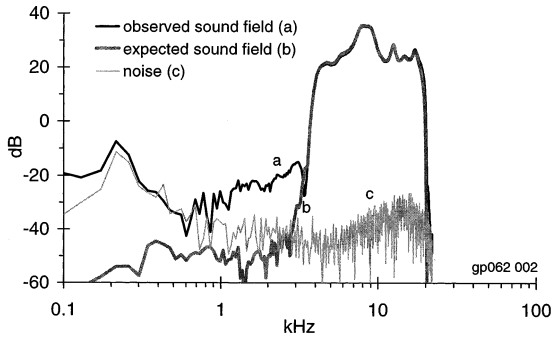

Fig. 4. Spectrum of the sound field recorded in the external meatus when stimulating with an uncompensated 4 kHz high-pass click. (a) The measured spectrum, (b) the spectrum expected from a linear ear, (c) noise level.

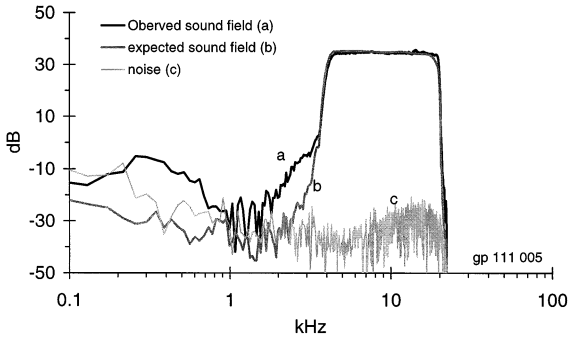

Fig. 5. Spectrum of the sound field recorded in the external meatus when stimulating with a frequency-compensated 4 kHz high-pass click. (a) The measured spectrum, (b) the spectrum expected from a linear ear, (c) noise level.

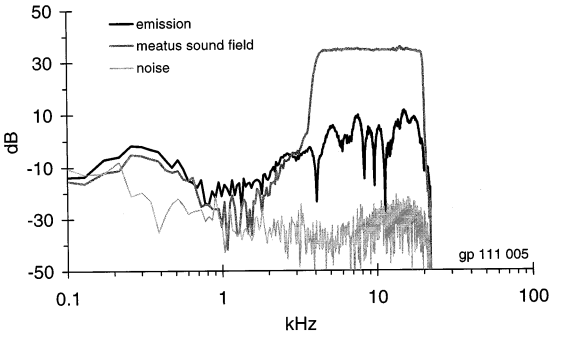

Fig. 6. Spectrum of non-linear-derived TEOAE. Also shown for comparison is the ear canal sound spectrum resulting from the probe click, from Fig. 5. The two spectra are of a nearly equal level outside the stimulus pass-band and there is no obvious discontinuity across the pass-band frequency, indicating that there is very little stimulus frequency emission within the stimulus pass-band.

in the frequency band below the band limit of the stimulus. This power, not originally present in the stimulus, can only have been produced by non-linear distortion and later evidence will demonstrate that this distortion was generated within the cochlea.

Clearly then, a high-pass click applied to the ear of the guinea pig results in the production of energy at frequencies not originally present in the stimulus. We now ask what the magnitude of this distortion is relative to the power of the differential non-linear emission. Even if there is distortion energy outside the click bandwidth, it might be small in comparison with stimulus frequency, channel-specific emissions within. Stimulus frequency-specific emissions are known to be evoked in guinea pig (Souter, 1995) and are therefore expected to be within the band limits of the click. Fig. 6 compares the spectrum of ear canal pressure in response to the high-pass click, with the corresponding non-linear-derived emission from the same frequency-compensated click. The most obvious point to be seen is that they are very similar in the range below 4 kHz and, in particular, there is no obvious discontinuity across the 4 kHz corner frequency. Although there is a general rise of emission power from low to high frequencies and there are a number of peaks and dips in this range, there is no obvious feature which would suggest that the emissions above and below 4 kHz are of a qualitatively different character. The dB scale on the abscissa of Fig. 6 may reduce the contrast across the transition band, but a change of 3 dB or so should be easily visible, so stimulus frequency emissions would appear from the figure to be smaller in magnitude than the contribution from the distortion products.

Fig. 7 makes a similar point with different data. Here, we compare two emissions derived from a wide-band click and a high-pass click. The two are very similar, although not identical, across the entire spectrum and below 4 kHz, there is little difference in absolute magnitude. In fact, the total power in the high-pass click emission is slightly greater (by 0.75 dB) than in the wide-band click and also over the 1–4 kHz range (by 0.42 dB). It is clear from this figure that the presence of stimulus power below 4 kHz makes negligible difference to the emission in that range, clearly demonstrating that little of the energy in that range was stimulus frequency-related. On the other hand, there are also small differences at higher frequencies, around 17 kHz, which is well above the click low-frequency band limit, showing that the low stimulus frequencies made some contribution to emissions even in this extreme range.

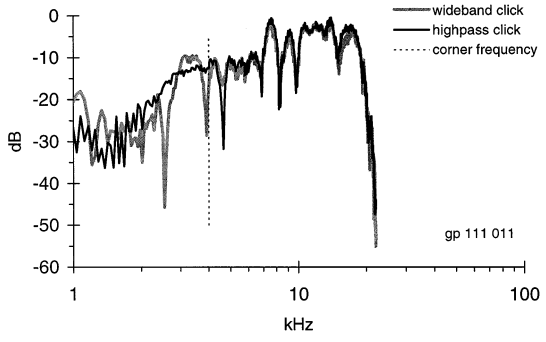

Fig. 7. Spectral comparison between emissions from a wide-band click and a high-pass click. The dotted line marks the nominal high-pass corner frequency of the click.

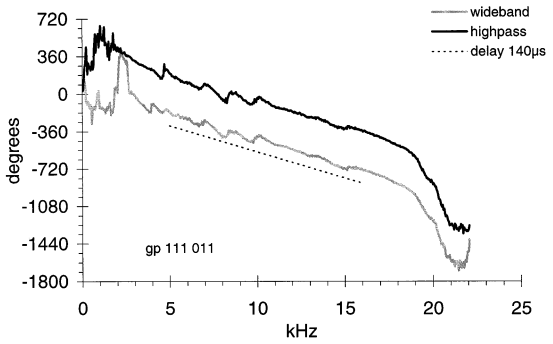

Fig. 8. Phase comparison between emissions from a high-pass click and a wide-band click. The dotted line indicates a slope of 140 μs.

These comparisons make it quite clear that virtually all the power present below 4 kHz in the wide-band non-linear-derived emission is intermodulation distortion. Furthermore, comparison of the emissions with the high-pass stimulus spectrum shows that there is no abrupt change in emission intensity at 4 kHz, as might be expected if there were extra stimulus frequency emissions in this range (see Section 4 for more on this point).

Fig. 8 shows phase responses for these two emissions.

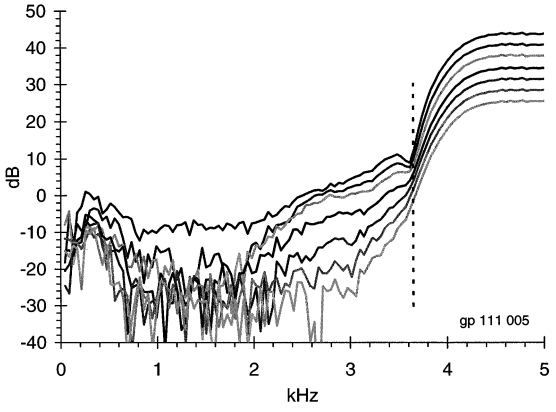

Fig. 9. Partial spectra for high-pass-filtered clicks at several intensities separated by 3 dB each. Note the restricted range of frequencies displayed. Above approximately 3.6 kHz (marked by the dotted line), the data are dominated by the stimulus spectrum, but below that, frequency intermodulation distortion dominates.

The lower curve (a) is the phase of the wide-band emission, while the upper curve (b) is the phase characteristic for the emission from the high-pass click, both after subtracting 1.95 ms delay to remove acoustical and software delays. Over most of the frequency range, there is virtually no difference between the phase responses, apart from two 180° shifts associated with notches in the amplitude spectra, again indicating that the 0–4 kHz band of the stimulus contributes little to the emission, even within that band.

3.5. Stimulus level dependence

The magnitude of the emission increased with stimulus click intensity. Fig. 9 shows the ear canal sound pressure spectrum in the region below 5 kHz for a high-pass click stimulus. There is a clear saturating growth in the spectral amplitudes with increasing stimulus intensity, although for a small band of lower frequencies, between 1 and 2 kHz, the growth is faster than linear or expansive. Fig. 10 shows the growth with the intensity of the total power in the derived emission, the power in selected spectral bands of the emission and the power in the frequency range 1–3.5 kHz for a 4 kHz high-pass click. The 1–3.5 kHz raw intermodulation energy initially grows faster than unity but tends to saturation at higher levels, while the derived emission

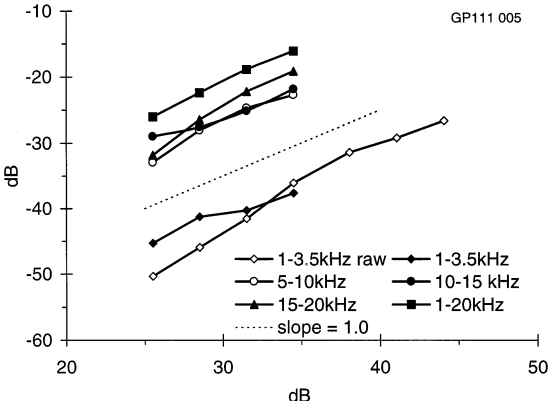

Fig. 10. Input-output function for power spectra of emissions in various frequency bands. Data are shown for derived emissions over the bands 1–20 kHz, 1–3.5 kHz, 5–10 kHz, 10–15 kHz, 15–20 kHz. Also shown are data for the spectral bands from 1 to 3.5 kHz for the unprocessed (raw) responses (open diamonds). The dotted line shows a slope of one for comparison.

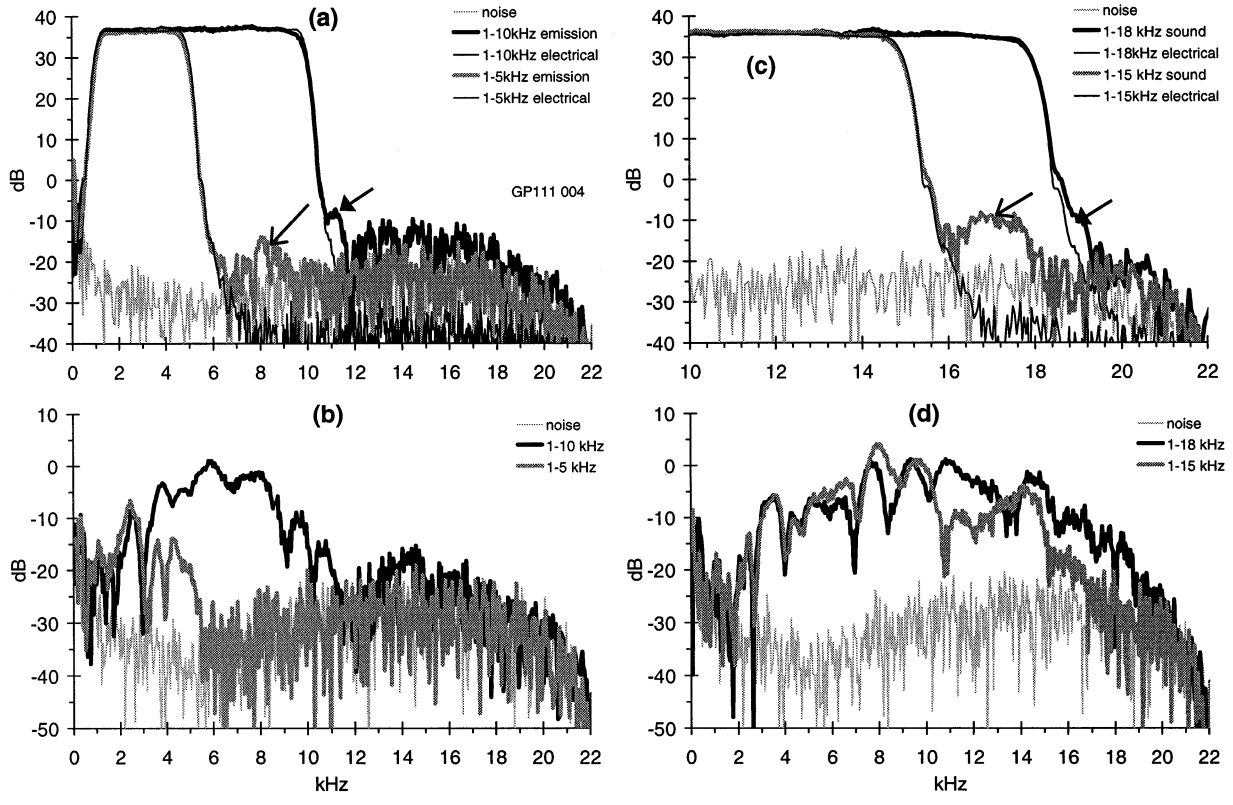

Fig. 11. Responses to band-pass clicks. (a) Spectra of sound in the external auditory meatus when stimulated with clicks of pass-band 1–5 kHz and 1–10 kHz. Intermodulation energy is clearly visible on the high side of the click pass-band for the 10 kHz stimulus (filled arrow) and barely for the 5 kHz click (open arrow). Also shown are the spectra of the electrical signals before frequency compensation and the spectrum of the noise. In each case, the electrical spectrum falls well below the noise level and well below the extended band of energy, associated with the 1–10 kHz click, extending out to almost 20 kHz. Note the linear frequency scale. (b) shows the two corresponding derived emissions, (c) and (d) show similar data for 1–15 and 1–18 kHz stimuli.

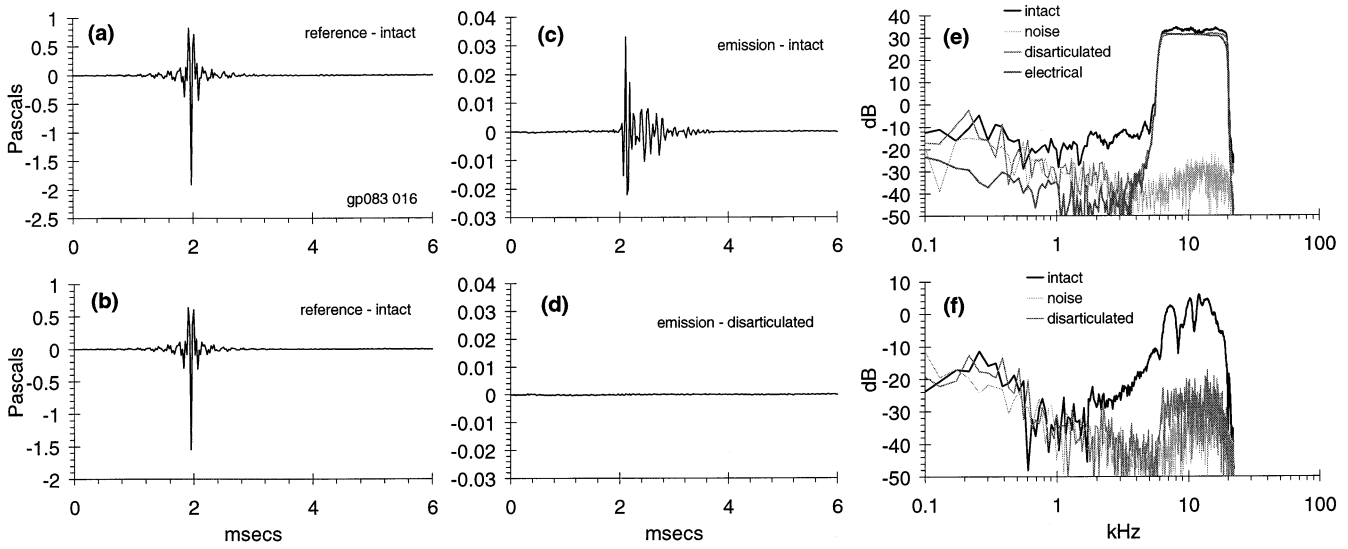

Fig. 12. Evidence that the emission is generated in the inner ear. (a) Reference click recorded in meatus, with the middle ear intact. (b) Reference click after disarticulation. (c) Non-linear-derived emission before disarticulation. (d) Emission after disarticulation. (e) Spectra of clicks in (a) and (b). Also shown are the noise level and the spectrum of the electrical signal (the latter being not visible because it coincides exactly with the post-disarticulation spectrum). Note the disappearance of the non-linear distortion in the range 1–4 kHz. (f) Spectra of the emission waveforms in (c) and (d), with noise also shown. Ordinate is Pa for a–d, dB SPL/Hz for e and f. Abscissa is ms for a–d and kHz for e, f.

appears to grow with a slope close to one for most bands, although the slope of the 15–20 kHz band appears to be greater than one at the lower intensities. This follows the previously reported trend towards greater compression for the lower frequencies, although in our case, the higher frequency bands often have a slope greater than one, as is the case for the 15–20 kHz band in Fig. 10.

3.6. Low-pass clicks

From a mathematical viewpoint, intermodulation should be produced at frequencies both above and below the stimulus frequencies, although previously reported distortion product emissions show a clear bias to lower frequency intermodulation products (Brown and Williams, 1993). This is probably because the interaction between the two primaries takes place at the characteristic site of the primaries. Intermodulation at lower frequencies will then be of a frequency below the local BM cut-off frequency and so should be able to influence the BM vibrations, while intermodulation at higher frequencies will be above the local cut-off frequency and so should not be able to influence the BM. Nonetheless, we should still expect to see some intermodulation at frequencies above the highest component frequency of the click and in fact, we do. Fig. 11 shows the meatal sound pressure for a set of low-pass clicks with successively lower corner frequencies. The two spectra in Fig. 11a are for 1–5 and 1–10 kHz clicks, while Fig. 11c shows 1–15 and 1–18 kHz clicks. Only a small amount of high-frequency intermodulation is evident in the 1–5 kHz click, but much more is evident in the 1–10 kHz click. The spectrum of the electrical stimulus, also shown in Fig. 11a, is just visible for both the 5 and 10 kHz clicks as a thin line lying behind the high-frequency slope. From there, it falls well below the noise level (shown in light gray). In Fig. 11c, the 1–15 kHz spectrum shows the greatest amount of intermodulation while the 1–20 kHz click shows relatively little, possibly because it was removed by the data acquisition anti-aliasing filters.

It is clear from Fig. 11 that intermodulation distortion is produced not only below the pass-band of the stimuli, but also above. Again, this is clear, unambiguous evidence for intermodulation distortion generated by the click, since it is well above the magnitude of noise or expected side-band response in that range.

Fig. 11 also shows, in b and d, the corresponding non-linear-derived emissions. It is clear from these figures that reducing the low-pass corner frequency reduces, but does not eliminate, the emission energy in the higher frequencies. Thus, in Fig. 11d, the emission from the 5 kHz low-pass click falls by approximately 15 dB at 5 kHz, but remains well above the noise floor beyond 15 kHz. The amplitude of the 10 kHz emission is greater by approximately 10–15 dB and extends up to about 10 kHz where it also falls to a reduced level but still well above the noise floor. A similar pattern is seen for the 15 kHz emission in Fig. 11d.

3.7. Confirmation of the cochlear origin of the emissions

We confirmed that the emission we recorded was of

cochlear origin in several ways. (a) We simulated an animal experiment using a small cavity, approximately the size of a guinea pig meatus, drilled in a block of plastic. Non-linear products were below the noise level of all recordings, both when the voltage to the loudspeaker was in the normal operating range and when the sound pressure in the cavity was similar to levels recorded in the animal. This eliminated both the loudspeaker and microphone as sources of distortion. (b) The delay between the click and the emission, although small, was clearly evident in the recordings (Fig. 2), indicating that the distortion was generated at least 150 μs after the click. (c) Phase analysis confirmed that the distortion followed the click by at least 150 μs (Fig. 3). (d) The emission and the intermodulation components all disappeared when the microphone probe tube was withdrawn a few mm from the meatus, although the stimulus changed by only a few dB. (e) The emission and the intermodulation components disappeared, albeit slowly, after the animal was killed, showing that it depended upon an energy source in the ear. (g) When the middle ear was disarticulated using a small probe, the stimulus changed by less than 1 dB over the click frequency band of 4–20 kHz, while the emission at all frequencies and the intermodulation distortion below 4 kHz were completely eliminated (Fig. 12). (h) When the cochlea was destroyed by pushing a metal probe through the round window and through the modiolus, without damaging the ossicular chain, all emission products disappeared immediately.

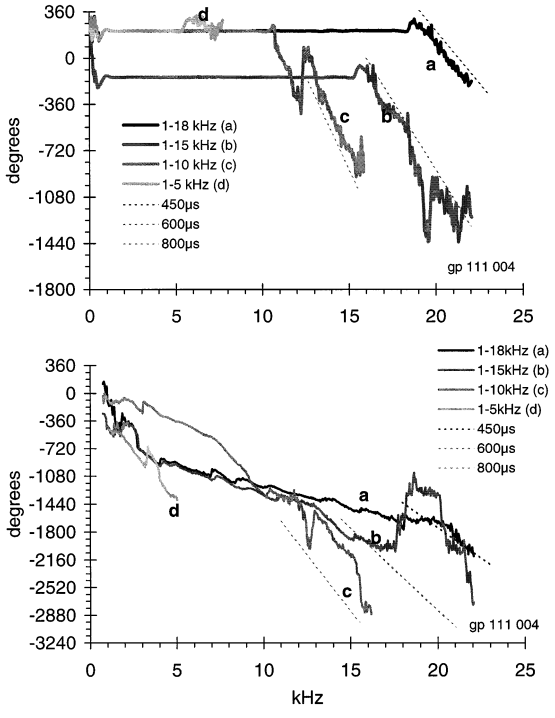

Fig. 13. Phase response for low-pass-filtered, compensated click for four band limit frequencies: 18, 15, 10 and 5 kHz. Also shown are lines with slopes of 450, 600 and 800 μs. Upper panel: raw sound. Lower panel: derived emissions.

As a result of the above checks, we were completely satisfied that the emission and the distortion components were generated within the inner ear.

4. Discussion

4.1. Stimulus intensities

The click stimulus intensities reported here may, at first sight, seem very large, being frequently larger than 1 Pa, or 94 dB SPL peak. They are also, however, of a very wide bandwidth and, particularly for the compensated stimuli, are of very short duration. Hence, the total power, or power per unit bandwidth, is typically within 10 dB of values reported by Kemp (1978). In general, it is very difficult to compare stimulus levels for transient stimuli, since changes in phase of the component frequencies of a stimulus can make dramatic changes in the peak amplitude. Furthermore, even comparisons of the spectral density are influenced by the duration of the analysis period, since the power is delivered in the first few ms but is quantified by averaging over the entire analysis epoch. In this paper, we show stimulus waveforms from which peak pressures may be read and we report spectra in units of dB re 400 μPa^2/Hz, averaged over a 23 ms epoch. These spectra units are identical with Kemp's dB SPL/Hz.

4.2. Evoked emissions

Transient-evoked emissions have, in the past, been very difficult to record from guinea pigs or other rodents (Wit and Ritsma, 1980; Schmiedt and Adams, 1981; Zurek, 1985; Avan et al., 1995) and when they have been recorded, they were of a very small amplitude (Zwicker and Manley, 1981; Ueda et al., 1992; Hilger et al., 1995). In this paper, we have described a click-evoked otoacoustic emission with several characteristics not previously reported: it is of very short latency, it has a very high intensity and it is of a very wide bandwidth. Furthermore, the emission was present in every individual animal that had CAP thresholds within the norms for our laboratory (13 in this study) and we have confirmed that the response is truly of cochlear origin.

Typically, emissions were evident after as little as 150 μs delay when wide-band clicks were used. Such short-latency emissions have been hinted before (Kruglov et al., 1997) and so should not be entirely unexpected, but they have not previously been demonstrated directly. This is due to non-linearities present in the hardware used by previous investigators, which resulted in uncan-

celled stimulus during the ringing period of the stimulus click. Of the successful attempts at recording any form of transient-evoked emissions from guinea pig, Zwicker and Manley (1981) reported latencies of 1.6–3.2 ms, Ueda et al. (1992) reported approximately 1 ms to onset, while Hilger et al. (1995) reported emissions beginning shortly after the 2 ms windowing period and peaking at about 4 ms.

Amplitudes also were different. Previously reported emissions range in peak sound pressure from 2 μPa (Zwicker and Manley, 1981, tone burst emission) up to 500 μPa (Ueda et al., 1992; Hilger et al., 1995), while our results show peak pressures up to 10 mPa. While our values are much greater, they are not necessarily inconsistent with earlier reports since their very short latency implies that they would have been eliminated from recordings in earlier studies by the windowing necessary to remove instrumentation non-linearities.

Finally, the spectral width of the emissions was far greater than anything previously reported for guinea pig. Again, instrument limitations may be the main reason for this, since the ILO series of instruments sample at a rate of 12 000 samples per second, limiting their recordings to an upper frequency of 6 kHz. Our system has a recording bandwidth of approximately 21 kHz. The spectra of emissions from both types of equipment, however, show similar peaks and dips, with a spacing of around 1 kHz, although the spectra of previously reported emissions appear to have more variable regions in which emission energy is small or entirely absent. Thus, the emission we describe appears not to have been described before, but is clearly related to the emissions which have been described in the past.

4.3. Intermodulation distortion in TEOAEs

The sound pressure measured in the external ear canal of the guinea pig when a high-pass click is presented clearly demonstrates that a significant amount of intermodulation distortion is produced within the cochlea when stimulated by a transient (Figs. 2, 4, 5, 11 and 12). In hindsight, this is not surprising, since such a stimulus includes a wide range of frequencies and it is clear from measurements of distortion product emissions (Lonsbury-Martin et al., 1987; Brown and Williams, 1993) that stimulation of the BM by two pure tones can generate additional spectral components not present in the original stimulus. Thus, we can envisage each spectral component in the click interacting with every other component to produce a range of intermodulation products. Judging from two-tone experiments, such interactions will be most efficient between spectral components separated by a frequency ratio of about 1.2 and such interactions will, depending on their amplitude, produce additional spectral components extending (mostly) downwards from their respective frequencies. Thus, a component at frequency, say, f_d, could have been generated by a number of possible interactions: by quadratic distortion from any pair separated by f_d or by cubic distortion by any pair f_1, f_2 related in frequency by the formula $f_d = 2f_1 - f_2$, or by a number of other possible interactions. Furthermore, the new energy will, in general, be produced with a different phase by each component pair and the nett amplitude will be a complex summation of a number of components, not generally in phase with one another. Thus, a given frequency in the emission could have been generated at almost any place in the cochlea more basal than its own characteristic place or for a small distance more apical. From what we know of two-tone intermodulation, however, we can expect that most intermodulation energy will be produced close to the characteristic places of the primary components and, since the distortion products are strongest for frequencies close to the primaries, close to the characteristic place of the distortion frequencies, at least for the lower stimulus intensities.

Fig. 9 supports this as it shows most of the new frequency components close to the edge of the stimulus spectrum for lower intensities and extending progressively to lower frequencies for higher stimulus intensities, exactly as happens with two-tone intermodulation (Brown and Williams, 1993). It is important to realize, however, that the spread of frequencies generated by this mechanism depends strongly on the stimulus intensity. At low intensities, DPOAEs are generated only for frequencies close to the primaries (approximately within one octave), while at higher stimulus intensities, a much wider range of frequencies is generated (Brown and Williams, 1993). Similarly, Fig. 9 shows that a relatively narrow range of intermodulation frequencies is generated by clicks of low intensity, but a much wider range is generated at higher intensities.

The data also show that intermodulation energy is not only present, but actually predominates in an emission (Figs. 2 and 6). If the intermodulation energy was just a small fraction of the total emission energy produced, we would expect a large difference between the spectral energy density above and below the click corner frequency. Below, we would expect only intermodulation energy and above, we would expect both stimulus frequency and intermodulation energy. This is clearly not the case, however, indicating that whatever frequency-specific emission energy is produced, it is not large in comparison with the distortion component. Furthermore, and as Figs. 9 and 10 clearly show, the rate of growth of the derived emission over the frequency range 1–3.5 kHz is similar in absolute magnitude to the 1–3.5 kHz intermodulation component in the raw sound field. Thus, we conclude that the non-

linear-derived transient otoacoustic emission consists predominantly of intermodulation distortion energy.

One final point to note is the general increase in intensity of the emission with increasing frequency for a frequency-compensated click, at a slope of about 6 dB/octave, up to approximately one octave below the high-frequency limit of the click (Figs. 2h, 6, 7, 12). The reasons for this are not clear.

4.4. Phase characteristics of the emission

Typically, the phase characteristics of the emissions are almost straight lines, except for a small region above and below the band limits of the click. The data of Fig. 3 show that, after adjustment of the time origin by about 1.95 ms to compensate for the stimulus delays, the stimulus phase is almost flat over the stimulus pass-band but exhibits an obvious slope above and below. We interpret this as showing that the energy outside the stimulus pass-band has a significant delay, in the order of 400 μs in Fig. 3. Furthermore, the emission phase shows an almost linear region over the pass-band range, with a slope of around 150 μs and an even greater slope outside. These delays, although highly significant in demonstrating a physiological origin for the emission, are much smaller than those previously reported (typically around 1–5 ms). They are, in fact, much more in line with BM delays (190 μs, Cooper and Rhode, 1992, 36 kHz CF; 700 μs, Robles et al., 1986, 7 kHz CF; 700–800 μs, Rhode, 1971, CF 8 kHz). In general, slopes are greater on the low-frequency side than on the high.

Delays for intermodulation distortion produced above the pass-band of frequency-compensated low-pass clicks varied with the band-edge frequency (Fig. 13) in a consistent manner, from 450 μs for the 18 kHz corner frequency to 800 μs for the 10 kHz cut-off. Again, these delays are consistent with the BM group delays for similar CF regions, suggesting that, for each cut-off frequency, most of the emission energy is being generated close to the characteristic place of the highest frequencies in the stimulus. This would also be consistent with the magnitude responses (Figs. 2h, 6 and 12) in which it is seen that the maximum emission amplitude is close to the upper frequency limit of the stimulus. An exception to this was usually seen when the stimulus was not frequency compensated. In these cases, the group delays indicated that the major component of the emission was originating at the place of maximum amplitude of stimulation. Thus, for Fig. 2a, the group delay was approximately 520 μs, corresponding well to the expected delay for 7 kHz, at which frequency a peak is clearly evident in the stimulus spectrum.

The linear characteristic of the phase curves indicates that much of the emission is generated with the same delay, implying again that the various frequency components of the emission do not reflect the operation of the cochlea at their own characteristic places, but rather that much of the frequency content is generated at a single place. Furthermore, the correlation of that delay with the upper frequency of the click indicates that that place is close to the characteristic place for the highest frequencies within the click.

4.5. Comparison with other TEOAE studies

Our results suggest that all frequency components of the guinea pig TEOAEs are generated either close to the region of the cochlea corresponding to the highest frequency in the stimulus, if the stimulus is substantially flat, or at the region corresponding to the frequency of maximum amplitude for uncompensated stimuli. This would not be inconsistent with previously reported results. Kemp showed that human cochleas with high-frequency loss generate emissions with reduced high-frequency components (Kemp et al., 1990) and this would be expected from our results. Damage to the cochlear amplifier basal of, say, the 4 kHz region of the cochlea would reduce the amplitude of vibration of the BM at that region and so reduce the amount of intermodulation distortion generated there and, since most intermodulation generated is of a frequency close to or lower than that of the generating frequencies, we would expect a drop in emission close to and below the 4 kHz region in the emission spectrum. This situation would be analogous to the experiments shown in Fig. 11 where we presented clicks with various low-pass cut-off frequencies. The corresponding emissions are generally restricted to below the stimulus corner frequencies, although there is a small amount of emission energy above the pass-band of the stimulus.

On the other hand, however, our results also are consistent with other, more paradoxical, reports. Along with a large reduction in the high-frequency emissions, we would expect changes (not necessarily reductions) in the low-frequency components of the emission (Withnell and Yates, 1998). Reduction of the BM vibration amplitude at almost any place along the cochlea would, especially at higher stimulus intensities, reduce the amount of low-frequency intermodulation distortion produced at that site and the nett emission amplitude at that lower frequency will be altered, either increasing or decreasing depending upon the phase interactions.

Thus, we can easily explain the results of Avan et al. (1993, 1995, 1997), provided only that we assume that the spectrum of the ILO-88 stimulus click extends significantly above the upper frequency limit of its recording capability, 6 kHz. Avan and his co-authors found, in both humans and guinea pigs, that damage to the

basal turn of the cochlea, affecting frequencies of 8 kHz and above, resulted in a loss of emission energy below 3 kHz. The ILO stimulus, however, is a single pulse of 80 μs width, band-limited only by an 11 kHz low-pass filter and sound delivery system and should contain significant energy out to that frequency. (We have confirmed this in our own measurements on an ILO-88.) Thus, according to our interpretation, the higher frequency components of the stimulus will be driving the more basal end of the cochlea and producing significant amounts of low-frequency intermodulation energy. Other lower frequency components of the stimulus will also be generating low-frequency intermodulation at more apical sites. Since the recording system registers emission frequencies only up to 6 kHz, the higher frequency components of the emission will not be recorded. When the basal turn is damaged, we argue, the reduced contribution of these higher frequency regions to the high-frequency emission will not be seen, because they are not recorded, but their contribution to the low-frequency emission will be reduced, apparently by enough to reduce the overall energy in the low-frequency components of the emission. Hence, the recorded TEOAE shows a loss of low-frequency power in response to damage at considerably higher frequencies.

Only the results of Prieve et al. (1996) might appear to contradict our interpretation. They used both wide-band and band-limited transient stimuli and compared the emissions from one-third octave-bands filtered from the responses to wide-band stimuli with unfiltered responses from narrow-band stimuli of corresponding frequencies. They found small but insignificant differences and concluded that the emissions were 'channel-specific', i.e. that the emissions from a wide-band stimulus were, over a given frequency band, genuinely representing activity from the corresponding place within the cochlea. Their narrow-band stimuli were, however, approximately one-half to one octave wide, providing plenty of opportunity for intermodulation to occur. Furthermore, and at the lower intensities at least, most of the intermodulation would be generated at frequencies similar to that of the stimuli so that we would expect little difference between the filtered wide-band responses and the narrow-band responses. In other words, their experiments were simply too insensitive to detect the difference between a channel-specific and an intermodulation response.

4.6. Comparison with human TEOAEs

Several differences have been noted between otoacoustic emissions recorded in humans and those recorded from rodents. The two most obvious are that (a) TEOAEs are smaller and of shorter latency in rodents than in humans and (b) DPOAEs are smaller in humans than in rodents. A further difference is that secondary emission of distortion energy appears to play a more significant role in the human cochlea.

In the light of our present results, we might be permitted to speculate that these differences are connected, in that the significant difference in both types of emission is in the degree to which secondary emission occurs. In humans, the DPOAE at frequency $2f_1-f_2$ appears to consist of two components (Brown et al., 1996; Brown and Gaskill, 1996; Heitmann et al., 1998). The first is attributed to emission of distortion energy from the site at which the two primary tones interact on the BM. It is then suggested that the energy produced at that stage propagates as a travelling wave to the characteristic place for the distortion frequency, where it excites the cochlear amplifier to again generate energy, this time as a stimulus-specific emission at the frequency of the distortion. The two sources of energy are different in time and space and so sum vectorially after propagating to and through the middle ear. Similarly, we might expect intermodulation energy produced by BM responses to a click stimulus also to propagate to their characteristic place on the BM and to produce re-emission of new energy from the cochlear amplifier. But, since the intermodulation energy is itself wide-band, we could expect the secondary emission to produce further intermodulation which might sum vectorially with the original distortion, albeit delayed by the time taken to propagate to the re-emission site and to excite the cochlear filter there. This process might then be repeated many times and as a consequence, we might expect a reinforced and prolonged TEOAE.

Rodents show little evidence of secondary emission of DPOAEs and, consequently, we might expect little re-emission of the TEOAE intermodulation energy produced by a click stimulus. Hence, we might expect smaller and shorter TEOAEs in rodents than in humans. But why should humans produce more secondary emission than rodents do? We have no ideas on this, other than that it might be related to the longer BM of the human, encoding a reduced frequency range and so allocating greater lengths of the BM to each frequency range. This might in turn permit greater independence of closely related frequency regions and hence more re-emission.

4.7. Implications for clinical use

The basic usefulness of the TEOAE as a simple pass-fail screening test for hearing loss is not altered by our interpretation of the phenomenon. If a subject being tested has a good hearing threshold in the range, say 1–6 kHz, this should usually be confirmed by the presence of a strong emission. On the other hand, if they

have poor thresholds across a range of frequencies, especially the higher frequencies, they will fail to generate a substantial emission. Even the presence of hearing loss confined to a band from, say, 4–6 kHz will presumably be reliably detected by the TEAOE response, since the emission will be somewhat reduced over that frequency range.

It is in the more subtle interpretations of the TEOAE response that we believe our results will prove significant. For example, we suspect that sensorineural loss of thresholds at frequencies across the lower range of approximately 1–3 kHz, admittedly the most unlikely situation, may be incompletely detected by TEOAE tests, because extrapolation of our results from guinea pig to human implies that much of the lower frequency energy in the emission may be produced by cochlear responses to (somewhat) higher frequency components of the stimulus. Thus, a loss from 1–3 kHz might not significantly affect the emission from an individual over that range because most of the emission in that range may have been generated by normal responses to the 4–10 kHz band of the stimulus. Conversely, some losses to the more basal turns of the human cochlea might result in apparent losses to the lower frequency components of the emission, suggesting a loss at low frequencies which is actually present at higher frequencies (Avan et al., 1993,1997).

Acknowledgements

This work was supported by the National Health and Medical Research Council, the Medical and Health Research Infrastructure Fund of Western Australia and the Department of Physiology of the University of Western Australia. R.H.W. was the recipient of a scholarship granted by the Department of Physiology.

References

Avan, P., Bonfils, P., Loth, D., Wit, H.P., 1993. Temporal patterns of transient-evoked otoacoustic emissions in normal and impaired cochleae. Hear. Res. 70, 109–120.

Avan, P., Bonfils, P., Loth, D., Elbez, M., Erminy, M., 1995. Transient-evoked otoacoustic emissions and high-frequency acoustic trauma in the guinea pig. J. Acoust. Soc. Am. 97, 1–9.

Avan, P., Elbez, M., Bonfils, P., 1997. Click-evoked otoacoustic emissions and the influence of high-frequency hearing losses in humans. J. Acoust. Soc. Am. 117, 2771–2777.

van den Brink, G., 1970. Experiments on binary diplacusis and tone perception. In: Plomp, R. and Smoorenburg, G.F. (Eds.), Frequency Analysis and Periodicity Detection in Hearing. Sijthoff, Leiden, pp. 362–373.

Bray, P., Kemp, D.T., 1987. An advanced cochlear echo technique suitable for infant screening. Br. J. Audiol. 21, 191–204.

Brown, A.M., Gaskill, S.A., 1990. Measurement of acoustic distortion levels reveals underlying similarities between human and rodent mechanical responses. J. Acoust. Soc. Am. 88, 840–849.

Brown, A.M., Gaskill, S.A., 1996. Suppression of human acoustic distortion product: dual origin of $2f_1$-f_2. J. Acoust. Soc. Am. 100, 3268–3274.

Brown, A.M., Harris, F.P., Beveridge, H.A., 1996. Two sources of acoustic distortion products from the human cochlea. J. Acoust. Soc. Am. 100, 3260–3267.

Brown, A.M., Williams, D.M., 1993. A second filter in the cochlea. In: Duifhuis, H., Horst, J.W., van Dijk, P., van Netten, S.M. (Eds.), Biophysics of Hair Cell Sensory Systems. World Scientific, Singapore, pp. 72–77.

Cooper, N.P., Rhode, W.S., 1992. Basilar membrane mechanics in the hook region of cat and guinea-pig cochleae - sharp tuning and nonlinearity in the absence of baseline position shifts. Hear. Res. 63, 163–190.

Elliott, E., 1958. A ripple effect in the cochlea. Nature 181, 1076.

Evans, E.F., 1979. Neuroleptanaesthesia: an ideal anaesthetic procedure for long-term physiological studies of the guinea pig cochlea. Acta Otolaryngol. 105, 185–186.

Heitmann, J., Waldmann, B., Schnitzler, H., Plinkert, P.K., Zenner, H., 1998. Suppression of distortion product otoacoustic emissions (DPOAE) near $2f_1$-f_2 removes DP-gram fine structure - evidence for a secondary generator. J. Acoust. Soc. Am. 103, 1527–1531.

Hilger, A.W., Furness, D.N., Wilson, J.P., 1995. The possible relationship between transient evoked otoacoustic emissions and organ of corti irregularities in the guinea pig. Hear. Res. 84, 1–11.

Kemp, D.T., 1978. Stimulated acoustic emissions from within the human auditory system. J. Acoust. Soc. Am. 64, 1386–1391.

Kemp, D.T., 1986. Otoacoustic emissions, travelling waves and cochlear mechanisms. Hear. Res. 22, 95–104.

Kemp, D.T., Brown, A.M., 1984. Ear canal acoustic and round window electrical correlates of 2f1-f2 distortion generated in the cochlea. Hear. Res. 13, 39–46.

Kemp, D.T., Chum, R., 1980. Properties of the generator of stimulated acoustic emissions. Hear. Res. 2, 213–232.

Kemp, D.T., Ryan, S., Bray, P., 1990. A guide to the effective use of otoacoustic emissions. Ear Hear. 11, 93–105.

Kim, D.O., Molnar, C.E., Matthews, J.W., 1980. Cochlear mechanics: Nonlinear behaviour in two-tone responses as reflected in cochlear-nerve-fiber responses and in ear canal sound pressure. J. Acoust. Soc. Am. 67, 1704–1721.

Kruglov, A.V., Artamasov, S.V., Frolenkov, G.I., Tavartkiladze, G.A., 1997. Transient evoked otoacoustic emission with unexpectedly short latency. Acta Otolaryngol. 117, 174–178.

Lonsbury-Martin, B.L., Martin, G.K., Probst, R., Coats, A.C., 1987. Acoustic distortion products in rabbit ear canal. I. Basic features and physiological vulnerability. Hear. Res. 28, 173–189.

Manley, G.A., 1983. Frequency spacing of otoacoustic emissions: a possible explnatation. In: Webster, W.R. and Aitkin, L.M. (Eds.), Mechanisms of Hearing. Monash University Press, p. 2.

Norton, S.J., Neely, S.T., 1987. Tone-burst-evoked otoacoustic emissions from normal-hearing subjects. J. Acoust. Soc. Am. 81, 1860–1872.

Prieve, B.A., Gorga, M.P., Neely, S.T., 1996. Click- and tone-burst-evoked otoacoustic emissions in normal and hearing-impaired ears. J. Acoust. Soc. Am. 99, 3077–3086.

Rhode, W.S., 1971. Observations of the vibration of the basilar membrane using the Mossbauer technique. J. Acoust. Soc. Am. 49, 1218–1231.

Robles, L., Ruggero, M.A., Rich, N.C., 1986. Basilar membrane mechanics at the base of the chinchilla cochlea. I. Input-output functions, tuning curves, and response phases. J. Acoust. Soc. Am. 80, 1364–1374.

Schmiedt, R.A., Adams, J.C., 1981. Stimulated acoustic emissions in the ear canal of the gerbil. Hear. Res. 5, 295–306.

Shera, C.A., Zweig, G., 1993. Noninvasive measurement of the cochlear travelling-wave ratio. J. Acoust. Soc. Am. 93, 3333–3352.

Souter, M., 1995. Stimulus frequency otoacoustic emissions from guinea pig and human subjects. Hear. Res. 90, 1–11.

Strickland, E.A., Burns, E.M., Tubis, A., 1985. Incidence of spontaneous otoacoustic emissions in children and infants. J. Acoust. Soc. Am. 78, 931–935.

Strube, H.W., 1989. Evoked otoacoustic emissions as cochlear Bragg reflections. Hear. Res. 38, 35–46.

Sutton, G.J., 1985. Suppression effects in the spectrum of evoked otoacoustic emissions. Acustica 58, 57–63.

Ueda, H., Hattori, T., Sawaki, M., Niwa, H., Yanagita, N., 1992. The effect of furosemide on evoked otoacoustic emissions in guinea pigs. Hear. Res. 62, 199–205.

Wit, H.P., Ritsma, R.J., 1980. Evoked acoustical responses from the human ear: Some experimental results. Hear. Res. 2, 253–262.

Withnell, R.H., Kirk, D.L., Yates, G.K., 1998. Otoacoustic emissions measured with a physically open recording system. J. Acoust. Soc. Am. 104, 350–353.

Withnell, R.H., Yates, G.K., 1998. Enhancement of the transient-evoked otoacoustic emission produced by the addition of a pure tone in the guinea pig. J. Acoust. Soc. Am. 104, 344–349.

Xu, L., Probst, R., Harris, F.P., Roede, J., 1994. Peripheral analysis of frequency in human ears revealed by tone burst evoked otoacoustic emissions. Hear. Res. 74, 173–180.

Zurek, P.M., 1985. Acoustic emissions from the ear: A summary of results from humans and animals. J. Acoust. Soc. Am. 78, 340–344.

Zweig, G., Shera, C.A., 1995. The origin of periodicity in the spectrum of evoked otoacoustic emissions. J. Acoust. Soc. Am. 98, 2018–2047.

Zwicker, E., Manley, G., 1981. Acoustical responses and suppression-period patterns in guinea pigs. Hear. Res. 4, 43–52.